Available online at www.sciencedirect.com
ScienceDirect
Journal of the European Ceramic Society 30 (2010) 1049–1057
www.elsevier.com/locate/jeurceramsoc

Synthesis of high-purity polycrystalline MAX phases in Ti–Al–C system through Mechanically Activated Self-propagating High-temperature Synthesis

A. Hendaoui [a,b], D. Vrel [a,*], A. Amara [b], P. Langlois [a], M. Andasmas [a], M. Guerioune [b]

[a] *LIMHP, UPR 1311 CNRS, 99 Avenue J.-B. Clément, 93430 Villetaneuse, France*
[b] *LEREC, Département de Physique, Université BADJI MOKHTAR, BP 12, 23000 Annaba, Algeria*

Received 17 August 2009; received in revised form 25 September 2009; accepted 1 October 2009
Available online 25 October 2009

Abstract

Ternary MAX phase compounds were synthesized using an alternative route called MASHS (Mechanically Activated Self-propagating High-temperature Synthesis). This original process combines a short duration ball milling (MA) of reactants (Ti, Al, C) with a self-sustaining combustion (SHS). The particle size evolution of the powder mixture during Mechanical Activation was monitored using XRD profile analysis. The effect of Al-excess was also discussed. XRD and SEM analyses have proved that the activation of the reaction kinetics must be accompanied by a decrease in the overall exothermicity in order to synthesize pure Ti–Al–C MAX phases by MASHS.
© 2009 Elsevier Ltd. All rights reserved.

Keywords: Powders-solid state reaction; Electron microscopy; X-ray methods; Microstructure-final; Carbides

1. Introduction

Ti_2AlC and Ti_3AlC_2, members of the novel ternary compounds, so-called MAX phases, have attracted considerable interest, primarily because of their unique properties combining many merits of both metals and ceramics.[1–6] Like metals, they show high thermal and electrical conductivity, and are easy to machine, resistant to thermal shock, and tolerant to damage. Like ceramics, they possess low densities, a high Young modulus, a low thermal expansion coefficient, high strength at high temperatures, and excellent oxidation resistance. All of these properties make Ti_2AlC and Ti_3AlC_2 promising materials for high-temperature structural and functional applications.

For preparing these ternary compounds, two kinds of methods are used nowadays. One is reactive sintering with proper starting reactants, including hot pressure (HP) sintering, hot isostatic pressure (HIP) sintering, and spark plasma sintering (SPS),[1–3] the other is combustion synthesis, also called self-propagating high-temperature synthesis (SHS), including either the use of elemental powders as raw materials[4,5] or aluminothermic process.[6]

Early work related to these phases using SHS, in the late '80s and early '90s[7,8] has been, if not completely disregarded, at least overlooked. One of the reasons may be the high residual phases' content, around 30%, that were found at that time in the final product, especially TiC when synthesizing Ti_3SiC_2, Ti_3AlC_2, and Ti_2AlC.[9] Other processes proposed around the same time, however, would systematically be more complex and include a purification step, which could have been proposed as a complement of SHS as well.[10] The residual TiC content at that time was about 5%.

Recently, a new variation of the SHS process was proposed by Gaffet et al.[11] The so-called MASHS (Mechanically Activated Self-propagating High-temperature Synthesis) process consists of a short duration high-energy ball milling step[12,13] followed by a self-sustaining reaction, or SHS (Self-propagating High-temperature Synthesis), where the starting sample, powdered or compacted, is heated at one end, thus igniting the exothermic synthesis reaction which self-propagated along the sample until this sample is completely converted. This process was applied successfully to produce nanocrystalline (30–35 nm) bulk FeAl intermetallic compacts with a relative density close to 80%.[14–16]

* Corresponding author.
E-mail address: vrel@limhp.univ-paris13.fr (D. Vrel).

0955-2219/$ – see front matter © 2009 Elsevier Ltd. All rights reserved.
doi:10.1016/j.jeurceramsoc.2009.10.001

In a previous paper,[5] as a preliminary study of the work presented here, we have shown that it is possible to improve the purity of the Ti_2AlC MAX phase obtained by SHS, by a control of various parameters, and specifically the heat losses: increasing heat losses by reducing the sample diameter, the purity of the MAX phases was improved. However, Mechanical Activation (MA) had to be used in order to prevent the quenching of the reaction front, i.e. to ensure the propagation of the reaction front in the whole sample.

In a first step, the objective of this study is to perform a thorough investigation on the influence of Mechanical Activation on the TiC content in the final products using the stoichiometric starting composition described by the following reaction:

$$2Ti + Al + C \rightarrow Ti_2AlC \quad (1)$$

In a second step we will focus on the influence of adding Al in excess relatively to Eq. (1) in order to reduce the amount of TiC in the final products. Al will be added by 0.5 mol steps to the as-milled powder presenting the higher reactivity, in order to provide the most extensive study: indeed, the most reactive powders is the hardest to quench, and thus can tolerate greater amounts of excess aluminum. Effects of Mechanical Activation (MA) and the Al-excess content will be analyzed as a function of phase conversion degree and combustion characteristics, including sustainability of the combustion wave and propagation rate of the reaction front. Using XRD analysis, the content of each Ti-containing phase in the as-synthesized product will be estimated.

2. Experimental

Samples were prepared from commercial powders of aluminum, titanium and graphite, which were carefully weighed on a precision scale (0.001 g) to obtain the compositions of the required stoichiometry. Aluminum powder is from Prolabo (99%, mean diameter 100 μm), titanium powder from Alfa Aesar (99.5%, <50 μm) and graphite from KgaA (99.5%, <50 μm).

Once weighed, the powders were thoroughly mixed using a Turbula® mixer, co-milled using a Fritsh® Pulverisette 6 planetary mill using agate vials and balls. The rotation speed of the disc was set at 250 rpm. The Ball-to-Powder weight Ratios (BPR, also called Charge Ratio, CR) and the corresponding milling time are given in Table 1. The as-milled powders were uniaxially cold pressed to give rectangular samples with dimensions of 4 mm × 8 mm × 14 mm and a relative density of 60%.

The resulting samples were then set in the reaction chamber, which is fully described in Refs. [17,18]. Ignition of the powder mixtures was then carried out under argon atmosphere, by a graphite plate heated up by a high intensity electrical current (up to 12 V to 200 A), which brought it to a temperature of about 2000 K, and the reaction was then analyzed by infrared thermography using an AVIO® TVS 2000 ST IR-camera.

X-Ray Diffraction (XRD) analysis has been performed using an XRG-3000 diffractometer from INEL. This diffractometer is equipped with a curved detector with a 90° aperture, thus working with an asymmetric Bragg–Brentano geometry; with a 50 cm curvature radius and 8192 digital channels, this detector provides a precision close to 0.01°. The radiation wavelength used is the Cu-kα_1 radiation, 1.54056 Å, monochromated by a germanium monocrystal; out of the two slits placed just before the sample, the one parallel to the linear beam is opened for only 13 μm in order to eliminate the Cu-kα_2 radiation. Pattern deconvolution was carried out by means of the profile-fitting program Fityk® to obtain parameters defining the position, height, integrated diffraction intensity, integral breadth and shape of individual Bragg reflections.

The contents of each Ti-containing phase formed in the as-synthesized product were estimated from the integrated XRD peak intensities according to the following formula:

$$W_X = \frac{A_X^{(h\,k\,l)}}{\sum_X A_X^{(h\,k\,l)}} \quad (2)$$

where W_X is the estimated fraction for one compound and $A_X^{(h\,k\,l)}$ its integrated diffraction intensity of the major peak of compound X, except for TiC, where the (1 1 1) peak, representing 80% of its most intense peak, the (2 0 0) peak, is used because other phases' peaks do not overlap it.

The micromorphology was observed by scanning electron microscopy using a JEOL JSM6400F scanning electron microscope.

Table 1
Characteristics of the different mixtures. From left to right: milling conditions; phases detected by X-ray analysis after milling; crystallite size ε_{Ti}; microstrain η_{Ti} (these last two parameters being estimated by Williamson–Hall plots); and measured propagation velocities.

Ball-milling conditions CR/Δt	XRD phases after milling	ε_{Ti} (nm)	η_{Ti} (%)	Propagation velocity (mm/s)
Turbula®	Ti, Al, C	–	–	30
10:1/2 h	Ti, Al, C	>500	–	32
10:1/4 h	Ti, Al, C	308	0.07	37
10:1/8 h	Ti, Al, C	308	0.17	80
20:1/2 h	Ti, Al, C	513	0.10	36
20:1/4 h	Ti, Al, C	154	0.18	Unsteady
20:1/8 h	Ti, Al, C, TiC	45	0.4	Unsteady
40:1/2 h	Ti, Al, C, TiC	81	0.12	43

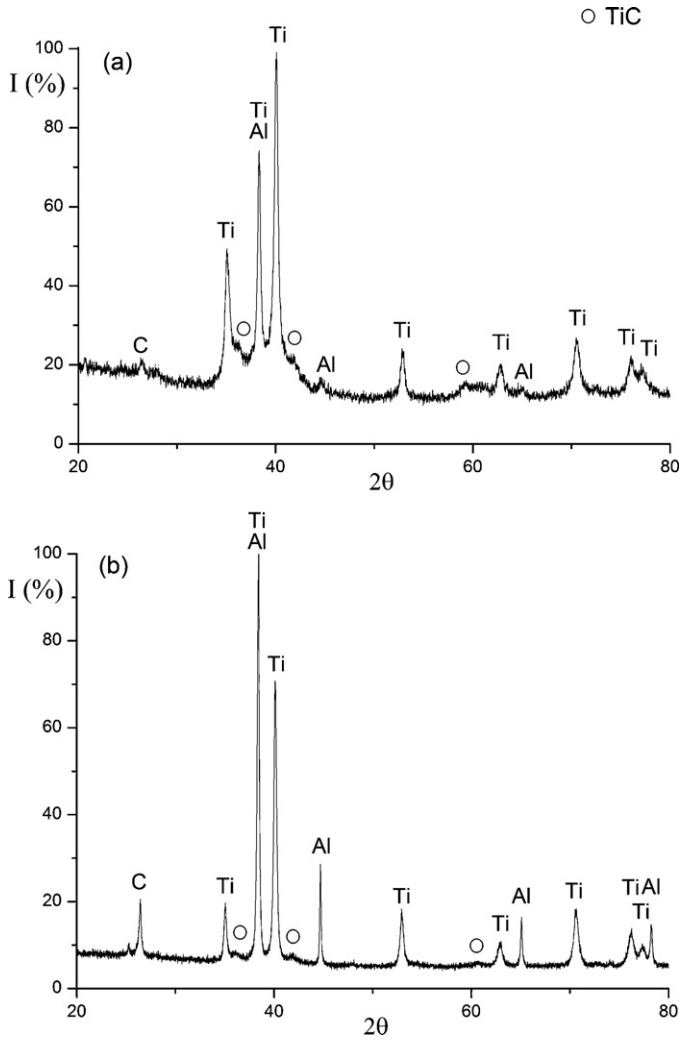

Fig. 1. Selected XRD patterns of as-milled powders: (a) 20:1/8 h and (b) 40:1/2 h milling conditions.

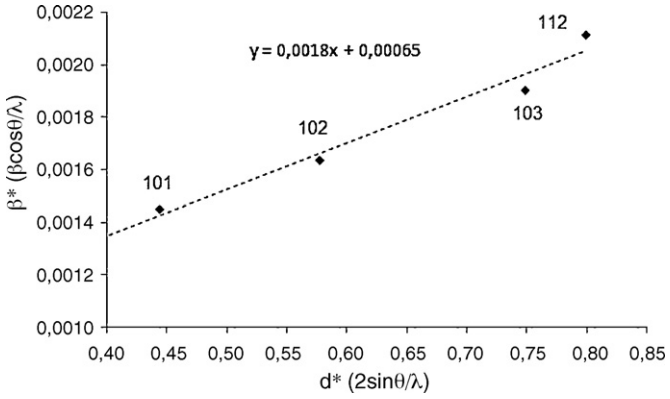

Fig. 2. Williamson and Hall plots for Ti grains in as-milled powders obtained in the case 20:1/4 h ball-milling conditions.

3. Results and discussion

3.1. Characterization of as-milled powders

3.1.1. Phases analysis

As shown in Table 1, mechanically activated powders are composed of the elements Ti, Al and C except for the 20:1/8 h and 40:1/2 h milling conditions, where production of TiC by mechanosynthesis can be detected (see Fig. 1). Fig. 1 shows also that the main peak of graphite is still present despite the beginning of mechanical alloying probably because the brittle graphite particles are dispersed in a ductile matrix of both metals, and thus, shock-induced amorphization of graphite which is observed when only Ti and C are co-milled[19] may therefore be less effective when aluminum is present. The production of TiC can be explained by the fact that at high CRs, because of an increase in the weight proportion of the balls, the number of collisions per unit time increases and, consequently, more energy is transferred to the powder particles and so alloying takes place faster. It is also possible that due to the higher energy, more heat is generated and thus could also change the constitution of the powder. A possible amorphous phase formed may even re-crystallize if the temperature rise is substantial.

3.1.2. Determination of crystallite size and microstrains from XRD profile line analysis

In order to calculate the average crystallite size and the microstrain of the sample, the change in the FWHM values for a series of Ti diffraction peaks at different values of 2θ was analyzed using the Williamson–Hall method.[20] It should be noted that this method relies on the difference between the FWHM peaks of the studied powder and the FWHM of a standard strain-free powder with large grain size, providing the instrumental peak broadening of the diffractometer. To obtain these parameters, pattern deconvolution was carried out using a Lorentzian profile shape, and unmilled Ti powder is used as a line broadening standard. The FWHM values for the unmilled sample are simply subtracted from the milled values when calculating the change in FWHM for the broadened peaks. Therefore, Williamson–Hall plots ($\beta^* = \beta\cos(\theta)/\lambda$ as a function of $d^* = 2\sin(\theta)/\lambda$) were used to determine the mean apparent crystallite size and the microstrain, given respectively by the y intercept and the slope of the straight line. A typical example of Williamson–Hall plots for Ti in the case of (20:1/4 h) ball-milling conditions is presented in Fig. 2.

Columns 3 and 4 in Table 1 present the evolution of crystallite size ε_{Ti} and the microstrain η_{Ti} obtained from Williamson–Hall plots versus ball-milling conditions for Ti in the as-milled powder. According to these results, a decrease in average crystallite size of Ti is observed when increasing milling time for a CR of 10:1 to reach an invariant submicron value of 308 nm after 4 h of milling. Faster and more important refinement of crystallites is observed for higher CRs, leading to nanosized Ti for 20:1/4 h, 20:1/8 h and 40:1/2 h milling conditions. These results are in a good agreement with previous studies showing that the CR has a significant effect on the time required to achieve a particular phase in the powder being milled[21]; the higher the CR, the shorter is the time required. In all cases, an increasing in microstrain with milling time is also observed.

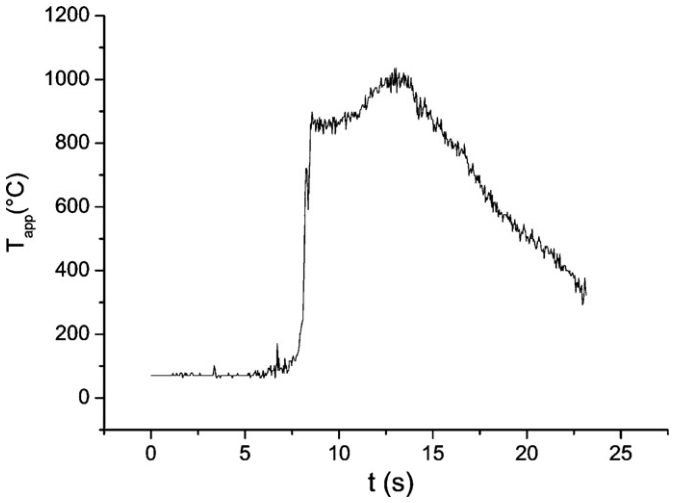

Fig. 3. Typical thermogram obtained from IR analysis of a SHS reaction for 2Ti + Al + C starting composition.

3.2. Self-propagating High-temperature Synthesis of the as-milled powders

From infrared image analysis, the thermal profile during the combustion reaction can be determined for several points on the sample (Fig. 3). Unfortunately, real-temperature values cannot be obtained from infrared measurements because the sample undergoes several phase transformations during the propagation of the combustion front, causing changes in emissivity. Moreover, the infrared camera needs the operator to set a value for this parameter, and we chose to arbitrary set it to 1; therefore, the temperature read by the camera is always strongly underestimated. Thus, we focused on the combustion front velocity to describe the reactivity of each powder: the higher the velocity, the higher the powder reactivity. Because the reaction may be accompanied by large volume change, the flame-front propagation velocity was determined from the delay for the wave to reach the end of the sample. The last column of Table 1 sums up the measured velocities versus ball-milling conditions. From these results, it seems that the crystallite size alone is not sufficient to characterize the reactivity of the powder, as the highest propagation velocity is not observed for the smallest grain size. Indeed, the propagation velocity of the combustion front can be influenced by a combination of many milling-enhanced parameters besides the reduction of the crystallite size,[22] e.g. the increase of number of contact surfaces,[23] the modification of balance energy during the self-sustaining reaction by the presence of a small amount of end product in the powder before reaction and by the stored enthalpy during mechanical treatment.[24]

The thermal profile during the combustion reaction in 2Ti + Al + C system exhibits a particular shape (Fig. 3), with an increase in the "apparent" temperature 2–3 s after the onset of the reaction front, probably due to the MAX phases' crystallization and a subsequent change in emissivity,[5] indicating that the formation process of MAX phases in the Ti–Al–C system is relatively complex. According to previous studies on quenched Ti–Al–C samples,[5] the reaction proceeds in three consecutive steps: first the formation of Ti-Aluminides, second the reaction of titanium with carbon giving sub-stoichiometric titanium carbide TiC_x, and then the reaction of TiC_x with melted Ti-Aluminides to form ternary Ti–Al–C compounds.

XRD patterns of the final products are presented in Fig. 4. 20:1/4 h and 20:1/8 h milling conditions did not permit a steady propagation and thus will not be considered. According to this figure, Ti_2AlC has been synthesized as the major composition. At the same time, the diffraction peaks of TiC are also visible. The presence of some supplementary diffraction peaks of α-Al_2O_3 in the case of 40:1/2 h milling conditions product indicates some oxidation probably induced by milling in open air (Fig. 4(c)). Surprisingly, the peak intensity corresponding to TiC appears to be weaker for the unmilled powder (Fig. 4(a)), implying a better degree of phase conversion for the sample with a lower reactivity.

The contents of TiC and Ti_2AlC formed in the as-synthesized product were evaluated by Eq. (2) based upon the XRD profile. Fig. 5 indicates that the estimated fraction of TiC yielded in the products from the elemental powder compacts is enhanced from 5.0 to 14.5%, as the front velocity increases from 3.0 to 8.0 mm s^{-1} due to Mechanical Activation. The unmilled powders gave the best yield in Ti_2AlC, estimated at about 95.0% (see Fig. 4(a)), while the most reactive powder, corresponding to 10:1/8 h milling conditions, gave the lower Ti_2AlC content, estimated at about 85.5% (Fig. 4(b)). According to a previous work,[5] this result is due to the high cooling rate of the small section sample by natural convection, coupled with low exothermicity of the unmilled powder. When the overall exothermicity (or the maximum temperature) increases, more TiC_x will be saturated with C and/or Al atoms will substitute C atoms in the sub-stoichiometric TiC_x before reaching Ti_2AlC and Ti_3AlC_2 temperatures of formation and thus will not react with Ti-Aluminides. As a result, some unreacted TiC_x will remain in the combustion products. Thus, the delay for the sample to reach the temperatures of the formations of the MAX phases during cooling from the combustion temperature seems to be a key parameter to control the TiC content in the final product: the shorter is the delay; the lower is the TiC content. This delay can be reduced, as we have done in previous studies, either by increasing the cooling rate[5] or by dilution.[6]

3.3. Effect of Al-excess on the phase formations

As 10:1/8 h milling conditions powder presents the higher reactivity, this study will focus on adding Al-excess to it as a diluent, in order to improve MAX phases yield in the combustion synthesis products. The compositions of the samples were selected from the Ti–Al–C ternary phase diagram,[25] which are shown in Fig. 6. The starting compositions, expected final composition and final crystalline phases in different samples are all listed in Table 2.

Addition of Al-excess gives rise the following three important consequences: (1) shift of the equilibrium to favor the reaction between TiC_x and Ti-Aluminides, yielding ternary compounds; (2) improvement in the liquid phase content during the exothermic reaction which favors the diffusion of the different

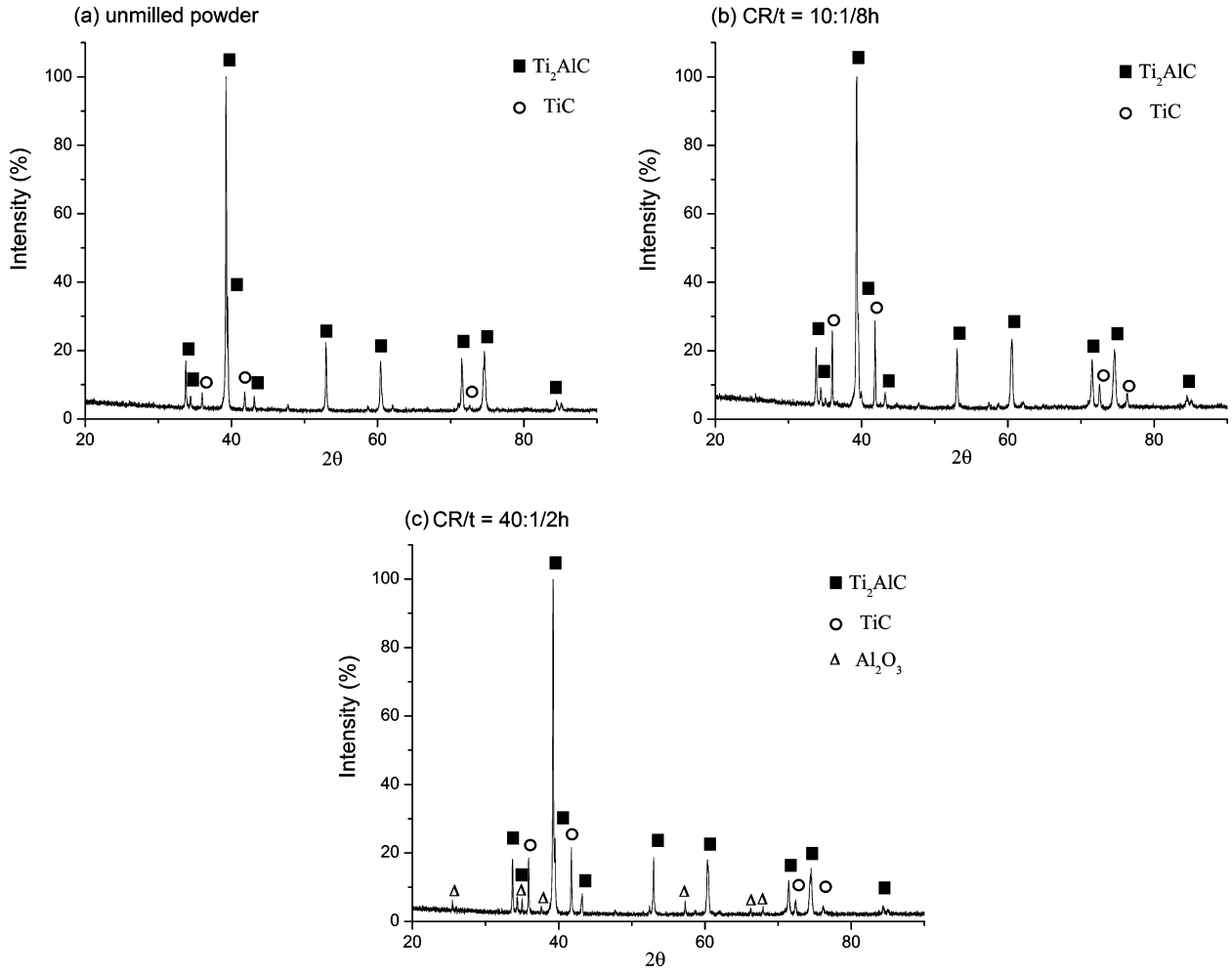

Fig. 4. XRD patterns of synthesized products obtained from different test specimens: (a) unmilled powder, (b) 10:1/8 h, and (c) 40:1/2 h milling conditions powders.

components, and thus promotes a better achievement of the reaction; and (3) dilution of the system therefore yielding a lower overall exothermicity.

Fig. 7 shows the XRD patterns of the products of the sample MA0, sample MA1, sample MA2 and sample MA3 (cf. Table 2). As a result of increasing Al-excess, a change in the TiC content of final products is observed. The dominant MAX phase also undergoes a change. The total MAX phases' content is also given in Fig. 8 from Ti_2AlC to Ti_3AlC_2. The corresponding evolution of the different Ti-containing phases' contents, evaluated by Eq. (2), is presented in Fig. 8 (dashed line). In this plot, two regions can be distinguished, according the evolution of total MAX phases' content:

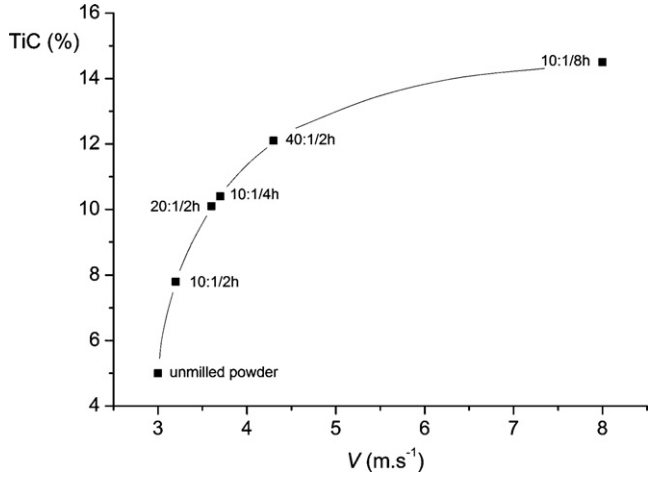

Fig. 5. Effect of Mechanical Activation on TiC content in the final products.

(a) For Al-excess ≤ 0.5 mol, a drastic increase in the total MAX phases' ratio with a decrease in remaining TiC content is observed. Naturally, when aluminum is added to a point that no ternary Ti–Al–C compound is rich enough to use it all, the overall exothermicity will decrease, and aluminum will therefore start to behave as a diluent, the temperatures of formation of MAX phases will be thus reached with more sub-stoichiometric TiC_x, which is chemically able to react with Ti-Aluminides to give the desired MAX phases. The total MAX phases' yield increases to reach a maximum value of 95.5% by adding 0.5 mol of Al-excess.

(b) For Al-excess > 0.5 mol, a decrease in the total MAX phases' yield is observed because of the disappearance of Ti_2AlC in favor of the production of another impurity, identified as $TiAl_3$. The minimum TiC_x content, estimated

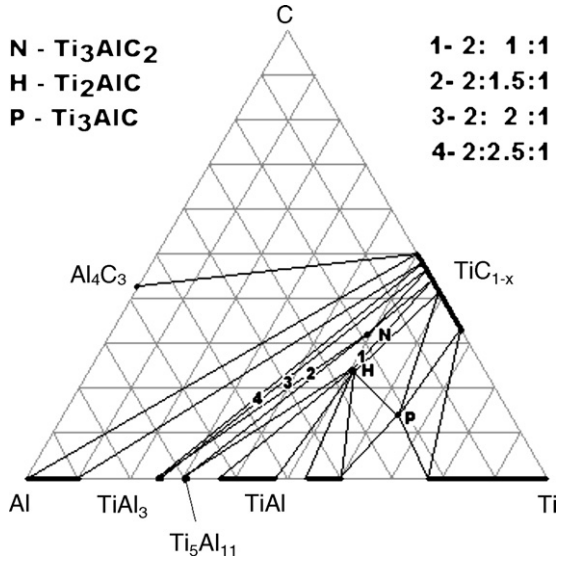

Fig. 6. Isothermal section at 1300 °C of the Ti–Al–C phase diagram.

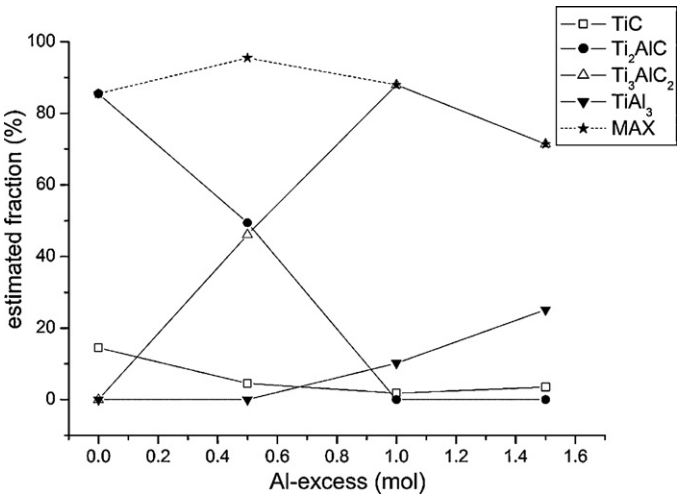

Fig. 8. Effect of Al-excess reactant compacts on estimation fractions of Ti_2AlC, Ti_3AlC_2, $TiAl_3$ and TiC formed in synthesized products from 10:1/8 h milling conditions powder.

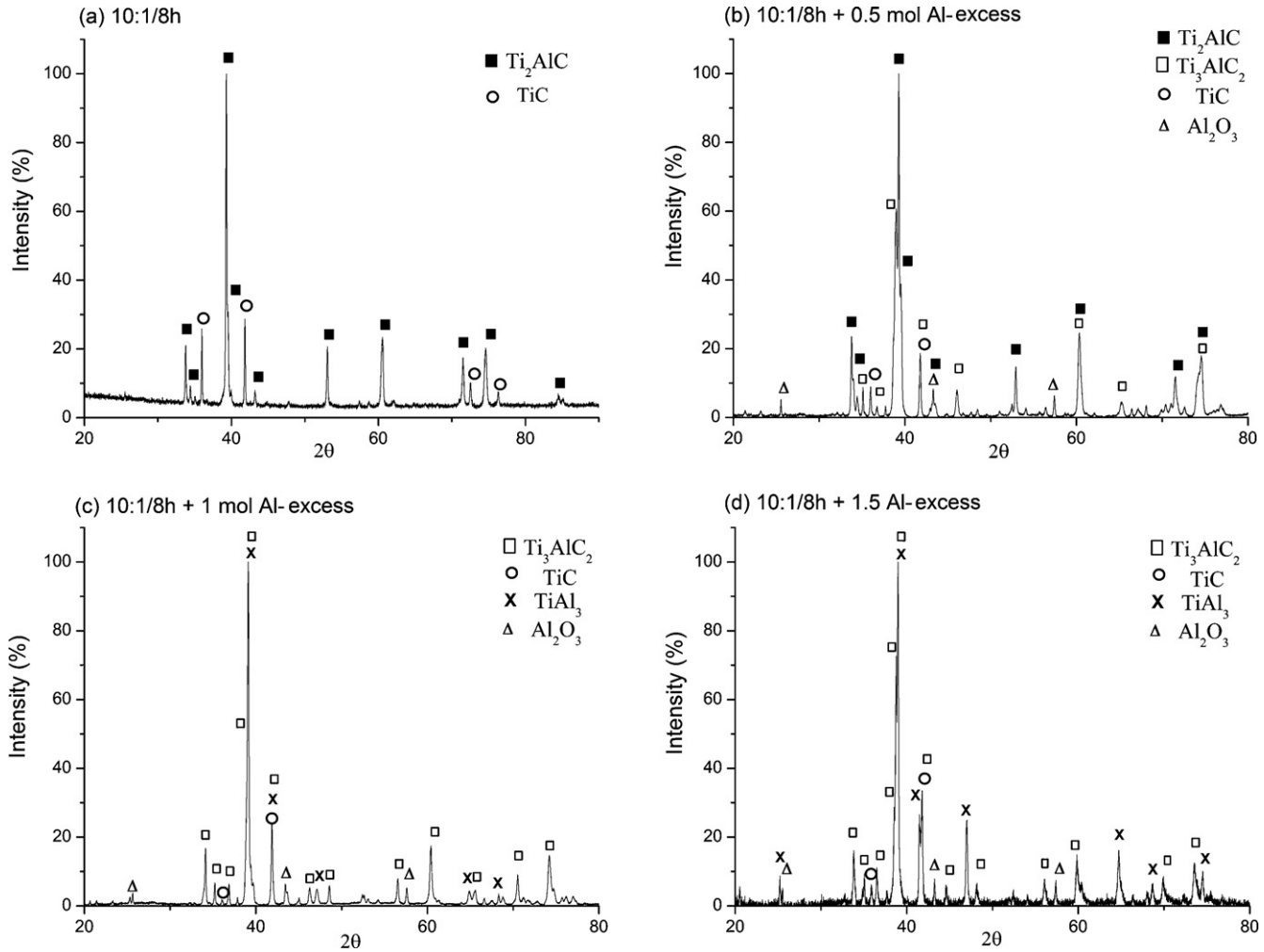

Fig. 7. Diffraction patterns of combustion products obtained from 10:1/8 h milling conditions powder with an Al-excess of: (a) 0 mol, (b) 0.5 mol, (c) 1 mol and (d) 1.5 mol.

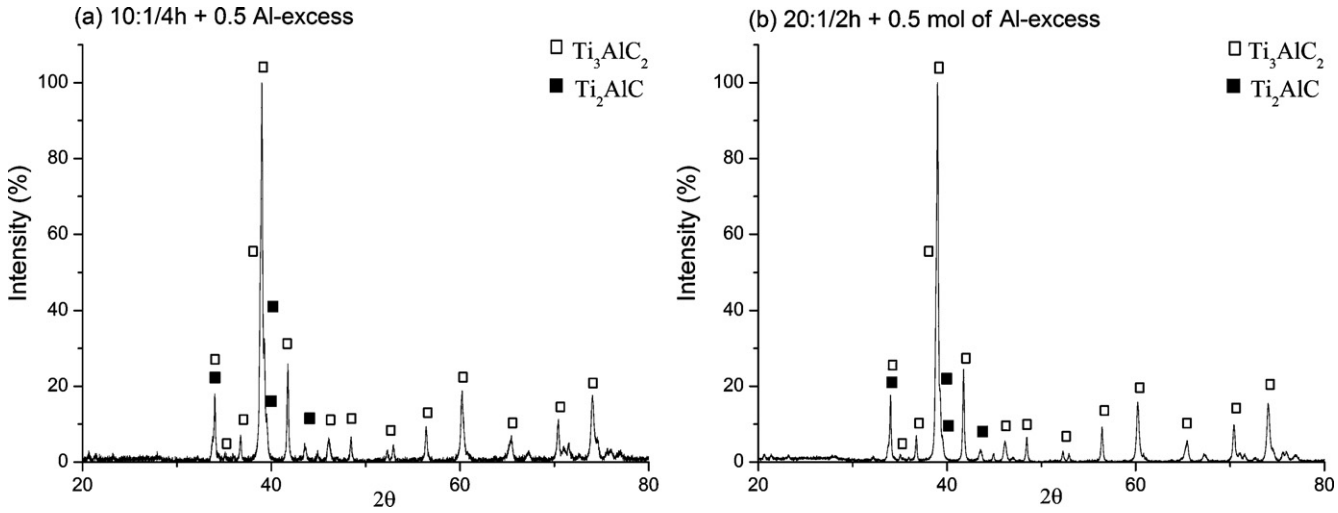

Fig. 9. Diffraction patterns of combustion products obtained from (a) 10:1/4 h and (b) 20:1/2 h milling conditions powders with an Al-excess of 0.5 mol.

at 1.8%, is obtained with 1 mol of Al-excess (i.e. sample MA2), is followed by a slight increase with decreasing exothermicity, probably due to a shorter time required for the synthesis of Ti_3AlC_2. In fact, the dilution effect is so important that the temperature of formation of Ti_3AlC_2 is not reached for a sufficient time to achieve the desired reaction between TiC_x and Ti-Aluminides, which tends to form a $TiC/TiAl_3$ composite instead of ternary compounds.

Although the method used here to estimate the amount of each phase could be questioned, as it is not as precise as a complete Rietveld analysis, it is sufficient for establishing some significant results: (i) MAX phases' total yield was improved for as-milled powders by adding Al-excess and (ii) the maximum yield ratio in MAX phases ($Ti_2AlC + Ti_3AlC_2$) is greater than 95%.

From these results, it would seem that the optimal value of Al-excess to add to 10:1/8 h milling conditions powder to obtain a complete disappearance of TiC without the formation of $TiAl_3$ is between 0.5 and 1 mol. However, when the same quantity of Al-excess (0.5 mol) was added to powders with lower reactivity, corresponding to 10:1/4 h and 20:1/2 h milling conditions, pure Ti_2AlC/Ti_3AlC_2 samples, with a total MAX phases' yield ratios greater than 99.5%, were obtained (Fig. 9(a) and (b)) where the peaks of the other phases are barely detectable. Consequently, the amount of Al-excess depends on the reactivity degree of the as-milled powder: the higher is the reactivity, the higher is Al-excess to add.

3.4. Products morphology

Typical SEM micrographs illustrating the fracture surface of synthesized products are presented in Fig. 10 for the sample MA0 and the sample MA2. Two different structures can be distinguished for sample MA0 (Fig. 10(a)): plate-like Ti_2AlC grains and small faceted TiC grains. MA2 product (Fig. 10(b)), exhibits layered structure characteristic of the Ti_3AlC_2 structure with a small amount faceted particles in some areas of the product which is the representative morphology of TiC. Moreover, another type of grains displays a solidified liquid morphology, probably due to the melting of Al during the reaction, characteristic of $TiAl_3$ phase.

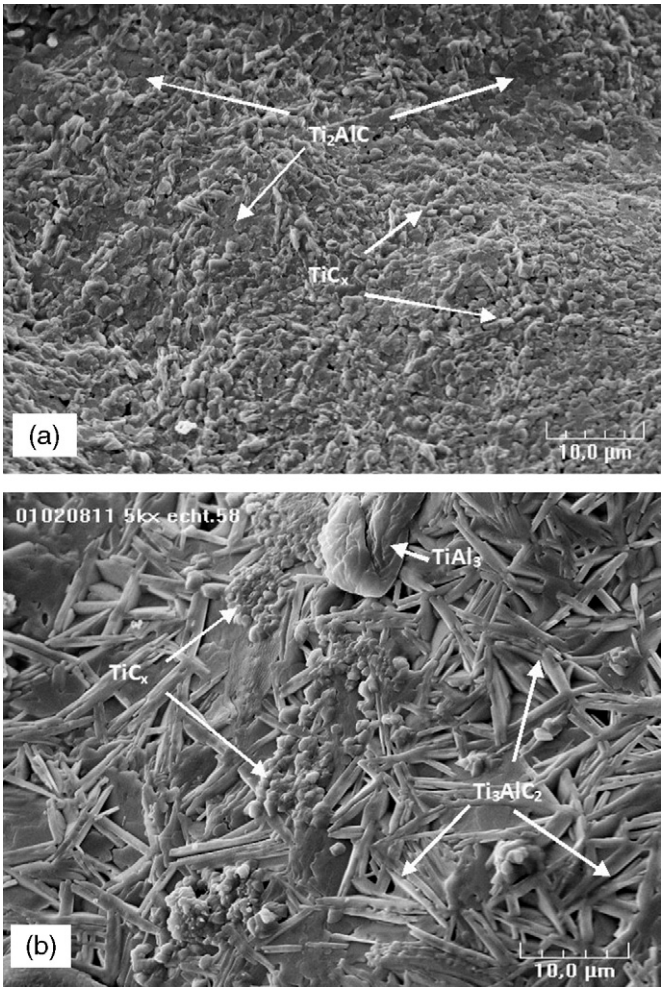

Fig. 10. SEM micrographs of synthesized products obtained from 10:1/8 h milling conditions powder with an Al-excess of (a) 0 mol and (b) 1 mol.

Table 2
The starting compositions, expected final composition and final crystalline phases in different samples.

Sample name	Stoichiometry (molar ratio) Ti:Al:C	Al-excess (mol)	Location in the phase diagram (cf. Fig. 6)	Experimental phases of the samples
MA0	2:1:1	0	H	H–TiC_x
MA1	2:1.5:1	0.5	N–$TiAl_3$–Ti_5Al_{11}	H–N–TiC_x
MA2	2:2:1	1	N–$TiAl_3$	N–$TiAl_3$–TiC_x
MA3	2:2.5:1	1.5	TiC_x–$TiAl_3$	N–$TiAl_3$–TiC_x

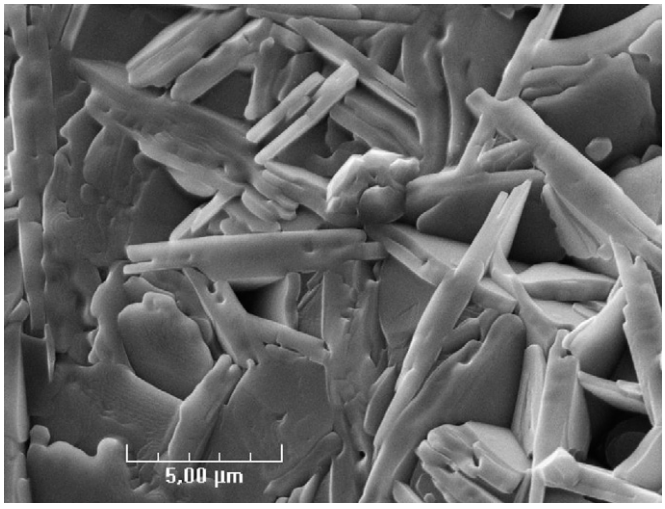

Fig. 11. SEM micrograph of synthesized product obtained from 20:1/2 h milling conditions powder with an Al-excess of 0.5 mol.

Fig. 11 shows the morphology of the 20:1/2 h milling conditions sample with 0.5 mol of Al-excess. The product is only made of plate-like Ti_2AlC and Ti_3AlC_2 grains with size of about 10 μm in length and 2 μm of width, which is in complete agreement with XRD results giving a total MAX phases' estimated yield of about 99.7% (Fig. 9(b)).

4. Conclusions

Mechanically Activated Self-propagating High-temperature Synthesis (MASHS) process was used to synthesize high purity Ti_2AlC and Ti_2AlC/Ti_3AlC_2 samples from Ti, Al and C elemental powders, with an estimated yield never obtained before with SHS process. From experimental evidences, the main conclusions can be summarized as follows:

(1) Despite a correct initial stoichiometry, TiC appears in the samples: TiC_x may be saturated with C and/or Al atoms may enter the TiC crystalline structure. For that reason, SHS is perfectly adapted to MAX phases, as it allows very short processing times, and thus can prevent the TiC_x saturation with C and Al in TiC substitution. Unfortunately, these are thermally activated processes, and the high temperatures reached during combustion synthesis may actually withdraw the advantage of the process.
(2) Mechanical Activation increases the reactivity of the as-milled powders and therefore the delay for the sample to reach MAX phases' formation temperature. Thus, TiC content in the final products is also increased.
(3) An efficient use of the SHS process to synthesize MAX phases should therefore come with a precise control of the delay for the sample to reach the temperatures of the formations of the MAX phases during cooling from the combustion temperature. The addition of Al-excess to as-milled powders allows such control. The amount of Al-excess depends of the degree of the reactivity of the powders.

In summary, activation of the reaction kinetic must be accompanied by a decrease in the overall exothermicity in order to synthesize pure Ti–Al–C MAX phases by MASHS. Fortunately, Mechanical Activation allows steady state propagation in conditions where dilution and/or heat losses are very high, greater than quenching threshold for unmilled powders, and the combination of these two parameters is enough to override the effect of heat increase due to Mechanical Activation.

According to the present work, addition 0.5 mol of Al-excess to 10:1/4 h and 20:1/2 h milling conditions powders seems to be a good solution to produce nearly pure Ti_2AlC/Ti_3AlC_2 MAX phases.

References

1. Tzenov, N. V. and Barsoum, M. W., Synthesis and characterization of Ti_3AlC_2. *J. Am. Ceram. Soc.*, 2000, **83**(4), 825–832.
2. Barsoum, M. W., Brodkin, D. and El-Raghy, T., Layered machinable ceramics for high temperature applications. *Scripta Mater.*, 1997, **36**(55), 535–541.
3. Zhou, A. G., Wang, C. A. and Huang, Y., A possible mechanism on synthesis of Ti_3AlC_2. *Mater. Sci. Eng. A: Struct. Mater.: Prop. Microstruct. Process*, 2003, **352**(1–2), 333–339.
4. Lee, W. C. and Chung, S. L., Ignition phenomena and reaction mechanisms of the self-propagating high-temperature synthesis reaction in the titanium–carbon–aluminum system. *J. Am. Ceram. Soc.*, 1997, **80**(1), 53–61.
5. Hendaoui, A., Andasmas, M., Amara, A., Benaldjia, A., Langlois, P. and Vrel, D., SHS of high-purity MAX compounds in the Ti–Al–C system. *Int. J. SHS*, 2008, **17**(2), 129–135.
6. Hendaoui, A., Vrel, D., Amara, A., Benaldjia, A. and Langlois, P., Ti–Al–C MAX phases by aluminothermic reduction process. *Int. J. SHS*, 2008, **17**(2), 125–128.
7. Pampuch, R., Lis, J., Stobierski, L. and Tymkiewicz, M., Solid combustion synthesis of Ti_3SiC_2. *J. Eur. Ceram. Soc.*, 1989, **5**(5), 283–287.
8. Lis, J., Pampuch, R., Piekarczyk, J. and Stobierski, L., New ceramics based on Ti_3SiC_2. *Ceram. Int.*, 1993, **19**(4), 219–222.
9. Chlubny, L. and Lis, J., Intermetallics as precursors in SHS synthesis of the Ti_3AlC_2. In *Proceedings of the IXth International Symposium on Self-propagating High-temperature Synthesis, Extended Abstracts Book*, 2007, pp. T3–12, edited by SF2M.
10. Racault, C., Langlais, F. and Naslain, R., Solid-state synthesis and characterization of the ternary phase Ti_3SiC_2. *J. Mater. Sci.*, 1994, **29**(13), 3384–3392.
11. Gaffet, E., Charlot, F., Klein, D., Bernard, F. and Niepce, J.-C., Mechanically activated SHS reaction in the Fe–Al system: in situ time resolved diffraction using synchrotron radiation. *Mater. Sci. Forum*, 1998, **269–272**, 379–384.

12. Gauthier, V., Josse, C., Bernard, F., Gaffet, E. and Larpin, J.-P., Synthesis of niobium aluminides using mechanically activated self-propagating high-temperature synthesis and mechanically activated annealing process. *Mater. Sci. Eng. A*, 1999, **265**, 117–128.
13. Gauthier, V., Bernard, F., Gaffet, E., Josse, C. and Larpin, J.-P., In-situ time resolved X-ray diffraction study of the formation of the nanocrystalline $NbAl_3$ phase by mechanically activated self-propagating high-temperature synthesis reaction. *Mater. Sci. Eng. A*, 1999, **272**, 334–341.
14. Charlot, F., Gaffet, E., Zeghmati, B., Bernard, F. and Niepce, J.-C., Mechanically activated synthesis studied by X-ray diffraction in the Fe–Al system. *Mater. Sci. Eng. A*, 1999, **262**, 279–288.
15. Charlot, F., Gaffet, E., Bernard, F., Klein, D. and Niepce, J.-C., In situ time-resolved diffraction coupled with a thermal i.r. camera to study mechanically activated SHS reaction: case of Fe–Al binary system. *Acta Mater.*, 1998, **47**(2), 619–629.
16. Charlot, F., Gaffet, E., Bernard, F., Gras, Ch. and Niepce, J.-C., Nanocrystalline FeAl synthesis by MASHS with in situ and post mortem characterizations. *Mater. Sci. Forum*, 1999, **312–314**, 287–292.
17. Vrel, D., Girodon-Boulandet, N., Paris, S., Mazué, J.-F., Couqueberg, E., Gailhanou, M. *et al.*, A new experimental setup for the time resolved X-ray diffraction study of self-propagating high-temperature synthesis. *Rev. Sci. Instrum.*, 2003, **73**(2), 422–428.
18. Bernard, F., Paris, S., Vrel, D., Gailhanou, M., Gachon, J.-C. and Gaffet, E., Time-resolved XRD experiments adapted to SHS reactions: past and future. *Int. J. SHS*, 2002, **12**(2), 181–190.
19. Heian, E. M., Karnatak, N., Vrel, D., Beaufort, M.-F. and Dubois, S., Effect of nanostructured reactants on TiC combustion synthesis and microstructure. *Int. J. SHS*, 2004, **13**(1), 1–12.
20. Williamson, G. K. and Hall, W. H., X-ray line broadening from field aluminium and wolfram. *Acta Metall.*, 1953, **1**, 22–31.
21. Suryanarayana, C., Mechanical alloying and milling. *Prog. Mater. Sci.*, 2001, **46**, 1–184.
22. Makino, A., Fundamental aspects of the heterogeneous flame in the self-propagating high-temperature synthesis (SHS) process. *Prog. Energy Combust. Sci.*, 2001, **27**, 1–74.
23. Gras, Ch., Vrel, D., Gaffet, E. and Bernard, F., Mechanical activation effect on the self-sustaining combustion reaction in the Mo–Si system. *J. Alloys Compd.*, 2001, **314**, 240–250.
24. Charlot, F., Bernard, F., Gaffet, E., Klein, D. and Niepce, J.-C., In situ time-resolved diffraction coupled with a thermal IR camera to study mechanically activated SHS reaction: case of Fe–Al binary system. *Acta Mater.*, 1999, **47**(2), 619–629.
25. Pietzka, M. A. and Schuster, J. C., Summary of constitutional data on the Al–C–Ti system. *J. Phase Equilib.*, 1994, **15**, 392–400.